DYNAMICS OF LINEAGE RESTRICTION FORMATION IN THE VERTEBRATE MIDBRAIN-HINDBRAIN BOUNDARY

An Undergraduate Research Scholars Thesis

by

BRIAN PATRICK KELLY

Submitted to Honors and Undergraduate Research
Texas A&M University
in partial fulfillment of the requirements for the designation as an

UNDERGRADUTE RESEARCH SCHOLAR

Approved by
Research Advisor: Dr. Alvin Yeh

May 2014

Major: Physics

TABLE OF CONTENTS

ABSTRACT

Dynamics of Lineage Restriction Formation in the Vertebrate Midbrain-Hindbrain Boundary. (May 2014)

Brian Patrick Kelly
Department of Physics
Texas A&M University

Research Advisor: Dr. Alvin Yeh
Department of Biomedical Engineering

Proper formation of lineage restrictions is important in developing animals to ensure healthy development. While mechanisms that form these restrictions are understood in invertebrates, it is not yet known what contributes to lineage restriction in vertebrates. We have used Ultrashort Pulse Microscopy to obtain 3-dimensional multimodal images of the developing midbrain-hindbrain boundary, a known lineage restriction in the zebrafish. By using this form of imaging, we have visualized both morphological and genetic parameters in this area and have used these to make quantitative and qualitative models of MHB morphogenesis and lineage restriction formation. These models allow us to have a better understanding of what exactly is responsible for the formation of the midbrain-hindbrain boundary and its lineage restriction in zebrafish with implications for all vertebrates, including humans.

DEDICATION

I would like to dedicate this thesis to my fiancé, Alison Simonetty, who has always been there for me through good and bad. This would truly not have been possible without her.

Also, I would like to dedicate this to my parents, Michael and Gail Kelly. They are truly my role models and their love and support have always inspired me to be a better person, both personally and professionally.

ACKNOWLEDGEMENTS

I would like to thank Holly Gibbs, who has spent many hours mentoring me and patiently guiding me through these projects. These accomplishments would not have been possible without her support.

Also, I would like to thank Dr. Alvin Yeh, my advisor, for helping me with my problems and guiding me through my projects and also for initially referring me to the undergraduate research scholars program.

Lastly, I would like to thank Dr. Arne Lekven, for always being supportive and allowing me to use his lab.

NOMENCLATURE

MHD – Midbrain-Hindbrain Domain

MHB – Midbrain-Hindbrain Boundary

MHBC – Midbrain-Hindbrain Boundary Constriction

TPF – Two-Photon Fluorescence

HPF – Hours Past Fertilization

GFP – Green Fluorescent Protein

UPM – Ultrashort Pulse Microscopy

CHAPTER I

INTRODUCTION

The zebrafish as a model organism

Many human diseases and disorders, including those in the nervous system, are developmental in nature. Whether it be genetic, morphological or both, it is important to understand the factors leading to such disorders and what may be done to prevent them. While it is important to study different factors that may cause diseases and developmental disorders, oftentimes it is hard to ethically do this in humans. As well, methods such as MRI or PET are great for producing some information relating to the causes of developmental disorders, but are also often lacking in their ability to paint complete causal pictures. Thus, other approaches are needed to able to study and understand exactly what goes on in the initiation and progression of these disorders. Model organisms allow us to fill in those gaps of understanding. By using model organisms, we can study processes that we could not traditionally study in humans, still giving us great insights into how diseases and disorders form but without doing any harm to humans. Thus, by studying model organisms, we can potentially come up with models and treatments for many important problems in modern medicine.

With that idea in mind, model organisms are an absolute necessity for many modern biologists trying to unravel these mysteries. They have allowed us, as a human race, to increase our knowledge of biology much further than would ever be possible studying humans alone. Model organisms have helped biologists in the past to discover essential things that can then be translated to human medicine – things such as how cells divide, how inheritance works and even how organisms process food into energy. There is a wide variety of model organisms, ranging

from single cell organisms, such as yeast, to much larger organisms, such as mice and guinea pigs. Different organisms, as well, are useful for different areas of biology – for instance, the common laboratory mouse (*Mus musculus*) is often used for translational medicine studies, while different types of yeast (single-celled fungi) are often used for genetic studies of basic biological processes such as cell division.

The zebrafish (*Danio rerio)* is a model organism common to areas of Southern Asia including India and Pakistan. Having the particular strength that its body is nearly transparent as an embryo, as illustrated in Fig. 1, the zebrafish is often used in studies of early internal anatomy and developmental genetics. Zebrafish are vertebrates; this is significant because many aspects of early development are evolutionarily conserved among all vertebrates. This means that research on zebrafish can then be related to humans through translational studies. Zebrafish embryos are popular not only because they can be easily studied genetically, but also because the embryos are easy to handle and produce. Female Zebrafish will often produce dozens of embryos at one time and can do this up to two or three times a week. Since the eggs are fertilized externally and the embryos grow externally, they can be observed at any stage to study different aspects of development. Zebrafish can be kept in large groups in tanks together and be separated when reproducing, and it is also possible to estimate the time that they will produce embryos (usually early morning), making it possible to precisely track developmental time periods. The ideal temperature range for zebrafish to develop is between 27° and 33° Celsius (80° to 91° Fahrenheit); this allows them to be handled and studied close to room temperature.

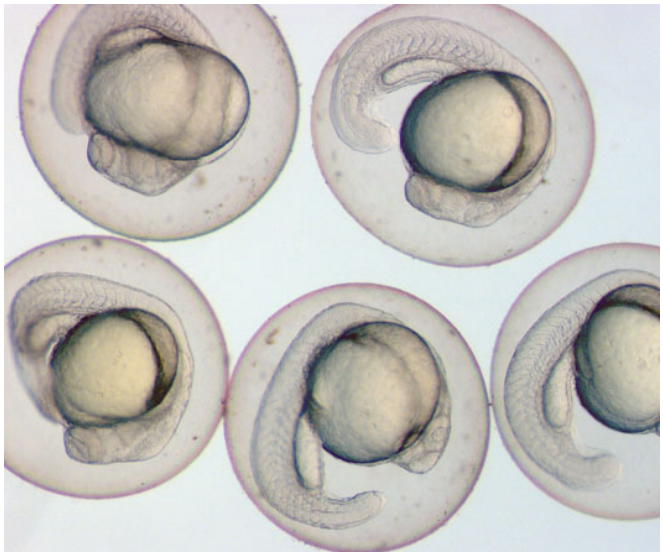

Figure 1. Zebrafish embryos within the segmentation period. The transparency of the embryos makes them ideal for visualizing internal structures as they develop. These embryos, including the chorion, are roughly 1mm in diameter.

This thesis focuses on a particular part of the zebrafish's nervous system called the Midbrain-Hindbrain Boundary (MHB). The MHB is located posteriorly in the zebrafish's brain and has a very distinct shape. The MHB is an invaluable tool for biologists because it allows them to study many aspects of biology and genetics that are conserved not only throughout all of this species, but often times throughout all vertebrates (including humans) as well. The MHB comprises the posterior midbrain and anterior hindbrain with a group of basally constricted cells in the center, known as the midbrain-hindbrain boundary constriction (MHBC). The MHBC begins to form at around 17 hours past fertilization (hpf) and continues to develop through about 24 hpf (Lowery 2008). However, while this time period is when the physical constriction begins to form, cell movements and gene expression patterns important to constriction formation are present from only a few hours after fertilization. Thus, it is important to study a wide range of times during development to get a full understanding of the physical and genetic mechanisms at play in the MHB.

While at first sight it looks simple, the MHBC is not strictly a group of constricted cells. It is also a lineage restriction – a precise boundary that does not allow cells of certain types to cross. Lineage restrictions such as the MHBC are extremely important in a developing organism because they allow compartments (groups of genetically similar cells) to form and thus establish a functional unit of genetic expression and morphological development in an organism. While many of the genetic and chemical mechanisms, such as a laminin-dependent basal constriction (Lowery 2008), leading to the physical formation of the MHBC are clear, there are no studies that have yet identified the cause of the lineage restriction at the MHBC. However, previous studies have found that Myosin II, a motor protein responsible for many aspects of cell motility, is responsible for establishment of lineage restrictions (like the MHBC) in the invertebrate fruit fly *Drosophila* (Landsberg et al., 2009), leading many biologists to suspect that Myosin II may also play a role in the zebrafish. Having a deeper understanding of the mechanisms that cause and reinforce these boundaries, especially in vertebrates, can lead to deeper understanding of how certain disorders begin and progress in humans and animals. For instance, in Barkovich *et al.* (2009), it is highlighted that many human neurological diseases can be tied back to morphological defects in the brainstem and cerebellum, which derive from the embryonic anterior hindbrain. By taking a reductionist approach to the study of MHB formation and understanding small, functional parts (like Myosin II) of the whole area, scientists can begin to get a better view of the full picture of MHB development and thus gain better insights with many practical applications in human medicine and development.

Oftentimes, studies done on the MHBC have the aim of further understanding genetic control of the morphological development of this area. While genetic studies are very important for this

area, studies accurately describing its morphological development can also be very useful, as they can give a greater insight into how gene expression in this area is translated from a chemical basis into a physical result. Many of the morphological studies done on the MHBC are qualitative in nature – they aim to describe what is happening with words and pictures as opposed to numbers. These studies are very important in describing how the relevant genes bring about a physical effect, and are often preferred since exact numbers are not always needed to give a detailed description of a biological process or mechanism. However, quantitative studies can offer strengths that qualitative studies sometimes lack. Quantitative data sets can allow one to accurately depict and predict how an area develops (to a certain error), giving scientists a standard system against which to compare certain measurements and outcomes. Ideally, a combination of qualitative and quantitative data can help scientists to gain a further understanding into a certain problem, as each approach will reveal different insights that might have been missed in the other.

Having a standard, quantitative system against which scientists can compare their data and experiments can allow for deeper understanding into how different genes and processes affect the MHB and to what extent they do. The experiments outlined in this thesis will offer both – qualitative data describing what is happening in the MHB as the experiments are performed, and quantitative data offering numbers and charts to precisely depict the descriptions. Both of these experiments will use Ultrashort Pulse Microscopy (UPM) to study different aspects of the MHBC with micrometer-level resolution, allowing high-precision measurements of this area. While one experiment will focus on setting up a framework against which to compare other

MHB studies, the other experiment will then investigate the effects that Myosin II and actomyosin cables have on the formation of the MHBC.

Specifically, I have measured different parameters at different depths in the MHB over time and used these to form a biological staging system as well as a functional description of MHB development. Also, I have tested how Myosin II affects the physical presence of the lineage restriction at the MHB. To do this, I have used Blebbistatin, a Myosin II inhibitor, to inhibit actomyosin cables from forming and tested how this affects the lineage restriction. While more work is needed, this project has allowed me to form a better understanding what may physically cause the lineage restriction at the MHB. Together, these studies can be used to describe some of the complex mechanisms leading to the formation of constriction and lineage restriction at the MHB.

Ultrashort Pulse Microscopy

Many biological experimentation techniques rely on using certain chemicals to bring about a reaction and then studying this to reach a conclusion. However, many times, these experiments need a way to visualize the results. For instance, if one wanted to see how an ultraviolet dye affected a small organism, he or she could apply it to the organism and then look at it under an ultraviolet microscope and take a picture. This is one such example of optical microscopy – the use of light to collect an image. There are many different types of optical microscopy, each having its own strength. For instance, if one wanted to see something (say, a zebrafish embryo) that was only one millimeter in size but completely viewable in normal light, they could use a simple dissecting microscope as opposed to a higher-tech imaging system. But if one wanted to

see something else in the embryo not visible with normal light – say, a fluorescent protein, then he or she would have to use a different system, such as a fluorescence microscope. Thus, depending on what is needed, different microscopy systems should be used to bring about different results.

The experiments described in this thesis used a form of microscopy called Ultrashort Pulse Microscopy (UPM). In UPM, one illuminates a sample with a femtosecond-pulsed laser beam, which then excites the tissue of the sample and causes it to release light. This light can then be collected by various methods and transformed into a digital image on a computer.
UPM is a very unique system in that it allows researchers to collect both structural and chemical information at the same time. By calibrating the laser system to excite specific molecules of interest and then collect their resulting signals, it is possible to acquire different images simultaneously from a single sample. Once these different images are collected, researchers can overlay them, allowing visualization of structural information and, with certain systems, visualization of several different molecules at once.

Probably the most important part of a UPM system is the pulsed laser source. To be discussed in the methods section, these pulses are the reason for many of the properties of UPM. For one, each individual pulse may have a high energy, but since they are so short in time, a sample does not have a long time to absorb them. Thus, as opposed to a traditional continuous wave laser at the same wavelength of light, ultrashort pulses can be used without doing any damage to a sample. The lack of damage allows a researcher to image an embryo *in-vivo*. UPM also allows for intrinsic optical sectioning, giving a 3-dimensional image that is extended up to a 2 mm

penetration depth in zebrafish embryos. Thus, UPM allows researchers to get high-resolution, micrometer-level 3-dimensional images while doing no harm to an embryo. Since the MHB is a 3-dimensional cellular-level system, UPM is an ideal system with which to study it, allowing for adequate resolution to quantitatively study the area and also allowing for simultaneous visualization of morphological structures and certain molecules.

CHAPTER II

METHODS

Sample preparation

These studies focused on two particular strains of zebrafish – standard wild-type embryos and a strain called *ecr20*, which expresses green fluorescent protein (GFP) in the MHB under the control of a transcriptional control region from the *wnt1* gene. Upon being fertilized, embryos were kept under standard conditions and staged using number of somites, as outlined in Kimmel *et al.,* 1995.

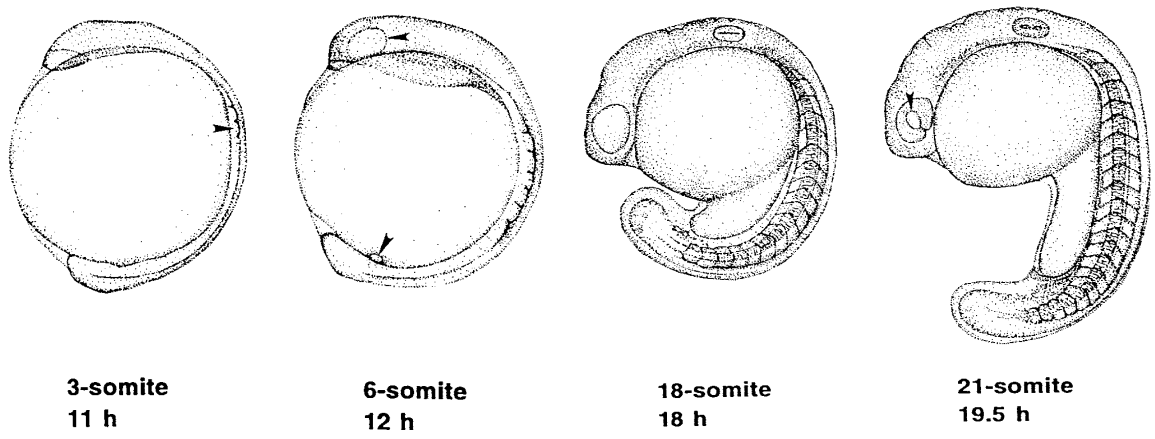

Fig 2 – Embryos from Kimmel's staging system, specifically those in the segmentation period. Used with permission from John Wiley & Sons out of the journal Developmental Dynamics.

Embryos used in the quantitative study of MHB development were wild-type embryos. After fertilization, these embryos were allowed to develop normally. The stages studied here were between the 10-somite stage (14 hpf) and 24-somite stage (21 hpf). For the current studies, embryos were imaged at time intervals spanning the formation of three somites. That is, we imaged them when they had formed 10, 15,17,21 and 24 somites. Variations in the time intervals, such as choosing 15 instead of 13 and 17 instead of 18, were used since these are morphologically relevant times in terms of development. As discussed in Lowery (2008), the

MHB begins to form the constriction at the 15 somite stage, and at the 17 somite stage the ventricles begin to open. Once the stage of development in which we were interested was reached, we imaged the still-developing embryo with the UPM system.

Embryos used to study the effect that Myosin II has on the lineage restriction boundary were raised up until the bud stage (10 hpf) before any somites begin to form. At this point in development, many important genetic and physical processes are happening in relation to the MHBC lineage restriction and the MHB as a whole. Upon reaching the bud stage, these embryos were treated with a 50μM solution of blebbistatin (a Myosin II inhibitor) in 0.05% Dimethyl Sulfoxide (DMSO) for three hours under otherwise normal development conditions. A control group of embryos in 0.05% DMSO in water was used under simultaneous treatment for comparison. After receiving the blebbistatin/DMSO treatments, the embryos were taken from the solutions and put back into normal water for further development. Upon reaching the desired stages of development within the segmentation period (10 hpf to 25 hpf) the embryos were fixed overnight using 4% Paraformaldehyde at 4° C and then rinsed with and stored in phosphate-buffered saline.

To image these zebrafish embryos on the UPM system, it was necessary to keep them still while also minimizing damage. We did this through a process called mounting. To do this, a layer of 1% agarose gel was poured into a petri dish and allowed to solidify. After solidifying, we would make a very small well in the agarose and insert a dechorionated zebrafish embryo, with a view of the MHB possible looking from straight above. Dechorionation is necessary to both maximize the optical signal and also to fit and adjust the embryo properly in the well. Upon inserting the

embryo into the well, we then covered it with another solution of 1.2% low-melting agarose, which has a higher transparency than traditional agarose gel and thus less optical signal attenuation. After allowing the low-melting agarose to solidify, the final step was to cover the mounted embryo in a few millimeters of water and then take it to the system to be imaged.

Imaging with ultrashort pulse microscopy

Ultrashort Pulse Microscopy allows us to collect high-resolution images that include both structural and chemical information about the sample that we are interested in. While several different mechanisms are possible, only one modality of UPM was used in our imaging – Two Photon Fluorescence (TPF).

Two-Photon Fluorescence

In order to induce fluorescence from an atom or molecule, a photon needs to match the energy necessary to excite an electron to an excited state. The energy of the electron is a result of the interaction of the electron with the atomic nucleus, among other things. The energy of a photon, however, can be described simply as:

$$\mathbf{E} = \frac{\mathbf{hc}}{\boldsymbol{\lambda}}$$

If a photon does excite an electron, this electron will then emit another photon of the same energy and consequently go back down to the relaxed state. With some previous knowledge about the energy of these gaps within the atoms, we can look at the emitted photon and identify the molecule of interest. Thus, we can get information about the molecules in a sample by

exciting the electrons within the atoms and collecting the photons these electrons emit. If only a single photon is used to excite an electron, it is called single-photon fluorescence.

Two-photon fluorescence follows a similar process as single-photon fluorescence, but instead of using a single photon of a certain wavelength to excite the atom, we can use two photons of double the wavelength, since:

$$\mathbf{E} = \frac{\mathbf{hc}}{\boldsymbol{\lambda}} = \frac{\mathbf{hc}}{\mathbf{2\lambda}} + \frac{\mathbf{hc}}{\mathbf{2\lambda}}$$

However, the electron that has now been excited by two photons will emit a single photon of half the wavelength of these two photons. A schematic of single-photon and two-photon processes is illustrated in Fig. 3.

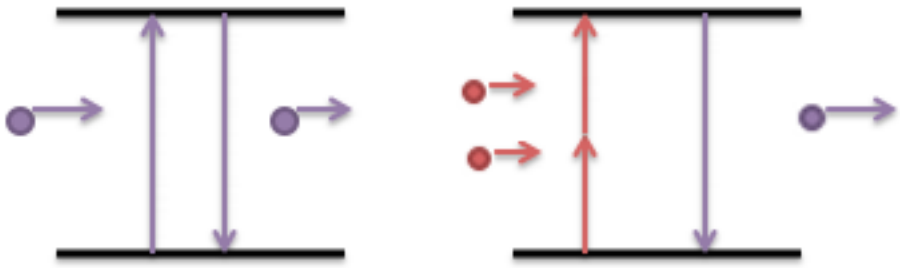

Figure 3. Left: a one-photon fluorescence process. A single photon of energy E is absorbed and excites an electron, the electron then emits a different photon of the same energy E. Right: A two-photon fluorescence process. Two photons, each of energy E/2, are simultaneously absorbed and excite a single electron. The electron then emits a single photon of energy E to go back to the ground state. The probability of this happening is much lower than a single-photon process.

Since TPF involves photons of twice the wavelength and thus half the energy, it allows us to excite a sample while doing much less damage to it than we would with single photons. Also, scattering in a sample is inversely proportional to wavelength, so a longer wavelength leads to less scattering in a tissue and thus a higher chance of interaction and signal collection. While two-photon fluorescence can provide a variety of advantages, the probability of it actually

occurring is very low. To compensate for this, we need a very high photon density, which is where ultrashort pulses come in.

Ultrashort Pulses

Ultrashort pulses are pulses of a laser that are very compressed in time. As a consequence of the Heisenberg Energy-Time Uncertainty Principle, these pulses must be spread out over a range of wavelengths. Our system uses pulses that have duration of less than 10 femtoseconds (10^{-15} s), resulting in a full-width half-max spread of about 130 nm, illustrated below in Fig. 4.

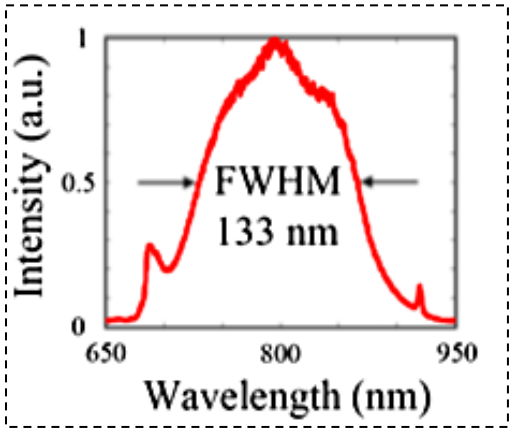

Figure 4. A normalized plot of the energy (wavelength) spread for a typical pulse. The pulse is center at 800nm (near-infrared region) and typically ranges between 650nm and 950nm.

Along with the spread in energy ranges, a single pulse from the laser will have a very high peak electric field intensity, corresponding to a very high photon flux. Pulsed lasers alternate between on and off at a certain repetition rate, often at the rate of millions of pulses per second. While this may seem like a lot of pulses, the time between pulses is actually about one billion times longer than the actual pulses themselves. Because of this, the laser is essentially off most of the time. Thus, while a sample may temporarily receive a high peak intensity from an individual pulse, the pulse itself does not last long enough for the sample to absorb a significant amount of energy.

Just as one would with any microscope, if we are trying to image a sample, we need to use a lens to focus the laser beam onto the sample. When a lens focuses a beam of light, it has a gradient-type effect on the intensity of the beam within the focus. The area in which the beam is focused is called the focal plane. As one moves outward from the focal plane, the intensity of the beam decreases. In a single-photon imaging system, it is possible to excite molecules at all points within the focus of the lens, not only at the focal plane. However, an ultrashort-pulsed laser such as ours will only have an intensity strong enough at the focal plane to reach the desired photon flux for a two-photon process. A consequence of this is that when an image is collected, it is only a two-dimensional "slice" of the area within the focal plane. However, as will be discussed, this can lead to 3-dimensional images by taking many of these slices and compiling them into one single stack.

Signal Generation

As discussed, we mainly utilize two-photon processes to collect data from the zebrafish. However, within the zebrafish, we are interested in two different signals coming from two-photon fluorescence. The first signal, called autofluorescence, comes from the interaction with metabolic molecules (pyridine nucleotides and flavins) within the mitochondria of the zebrafish cells (So, 2009). Since this signal will come from every cell within the zebrafish, we can use it to form an image of the actual morphology of the embryo. The second signal comes from the interaction with green-fluorescent protein (GFP). For the projects, as discussed earlier, we used a transgenic line of zebrafish with GFP incorporated in genetic sequence of the strain, called *ecr20.* This GFP will be expressed whenever certain lineage-restricted cells within the MHB express the *wnt1* gene, allowing us to collect data over cell proliferation at the MHB. By

combining autofluorescence and the signal from GFP, we are able to get morphological and biochemical data at the MHB.

The Imaging System

When actually getting images, it is important to optimize our laser system to be able to excite the molecules that we are interested in and also to collect the signals that we are interested in. To do this, we have to be able to do several things including: making and shaping the pulse correctly, compensating for dispersion, properly exciting the sample and properly collecting the signal. A simplified schematic of the system and its components is depicted below in Fig. 5.

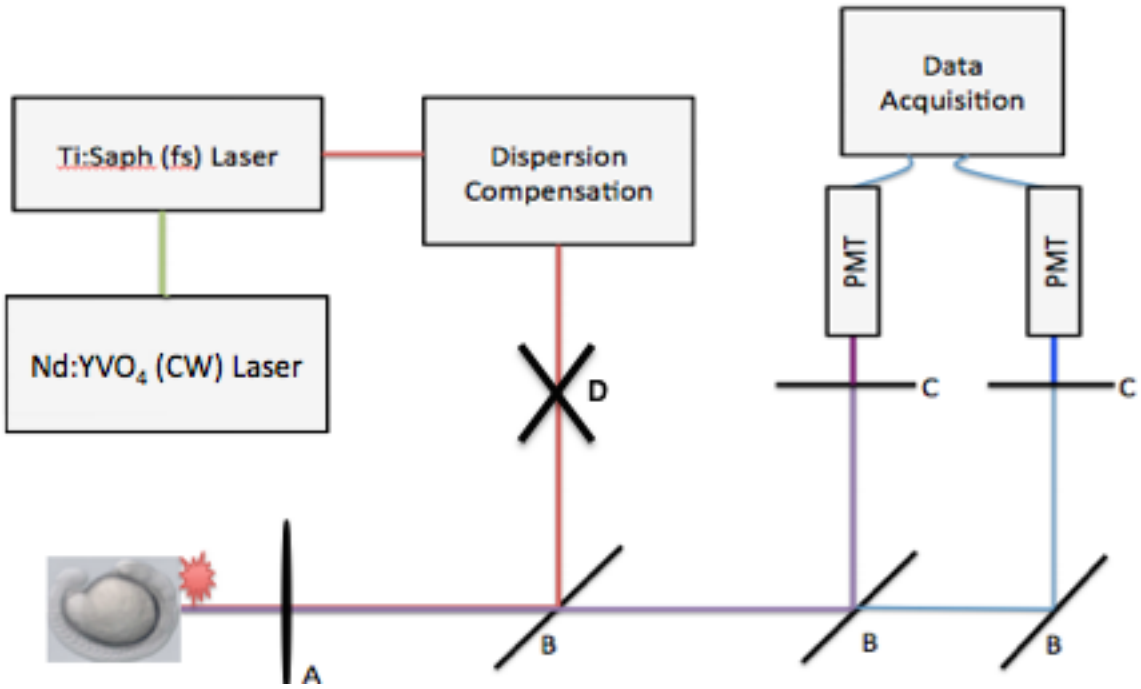

Figure 5. A schematic of the UPM system. A: The apochromatic water-immersion objective lens used to focus the initial pulsed signal and collect the fluorescence signal. B: Dichroic mirrors used to filter components of the fluorescence signal. C: Band-pass mirrors used for further filtering and refinement of the fluorescence signal. D: Galvanometer-driven xy scanning mirrors are used to scan the focused beam across the sample.

Making and Shaping the Pulse

As illustrated in the schematic, the excitation signal starts with a Neodymium-doped yttrium-Vanadate (Nd:YVO_4) laser (Coherent). The continuous wave from the Nd: YVO_4 laser is directed into a Titanium-doped Sapphire (Ti:Saph) laser (Femtolasers) where it interacts with the crystal, producing a new light beam around 800 nm, in the near-infrared region of the spectrum.

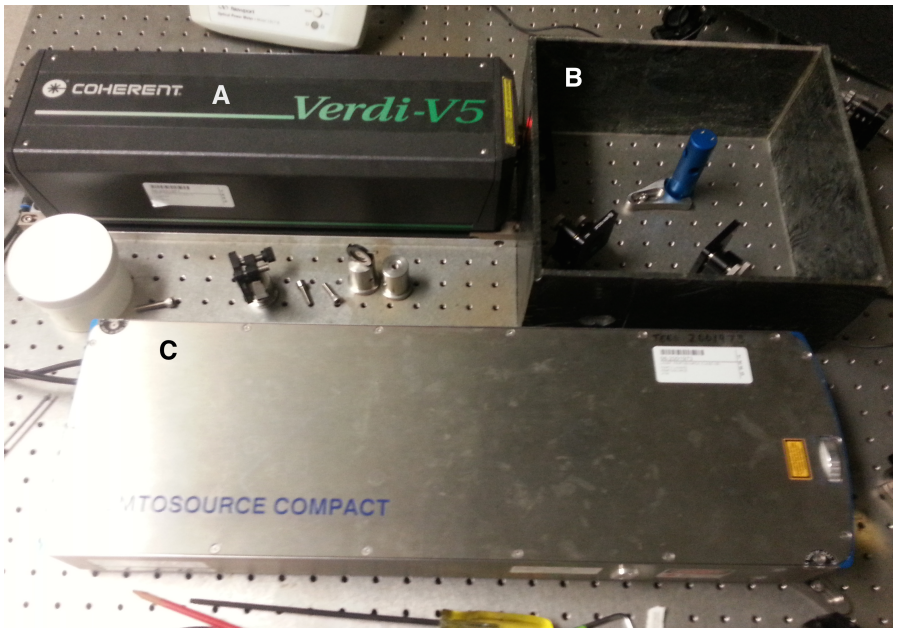

Figure 6. A: The Nd:YVO_4 continuous-wave laser. B: A periscope used to adjust the elevation of the Nd: YVO_4 beam to the level of the Ti:Saph laser. C: The Ti:Saph laser which will emit a pulsed beam.

Once the new beam is produced, it undergoes a process called mode locking in which a specific phase relationship between different parts of the beam is produced. This phase relationship then causes destructive and constructive interference at different parts of the beam, producing the pulsed profile that will be used to image the sample.

Since the index of refraction of the medium (air) that the pulse will travel through depends on the wavelength of light, this pulse will be subject to a wavelength-dependent dispersion, similar to light in a prism. This phenomenon, known as group-velocity dispersion (GVD), will cause the pulse to broaden in time, decreasing the peak intensity of the pulse and thus decreasing the efficiency with which we can excite the sample. GVD happens because the shorter wavelengths

of light will travel more slowly through the medium than the longer wavelengths contained in the pulse. To make up for this inevitable dispersion, we must use a set of dispersion-compensating mirrors, made by Femtolasers. These mirrors produce an opposite effect of air. Using a special thin-film coating, the mirrors cause the longer wavelengths to travel more slowly, allowing the shorter wavelengths within the pulse to catch up, restoring the original pulse profile. Once the pulse passes through the dispersion-compensating mirror set, it travels through a set of x-y scanning mirrors (to be discussed later) and into the microscope.

The Microscope

The microscope (Zeiss Axioskop 2) is equipped with ports for various filters as well as having room for two photomultiplier tubes, which are used to actually collect the data. A dichroic mirror reflects the beam into a specialized apochromatic water-immersion objective lens. This lens serves to focus the beam, allowing us to get necessary intensity for two-photon excitation at the focal plane. Being water-immersed, the lens will have a higher numerical aperture than simply being in air, and longer working distance (about 2 mm). When imaging within the focal plane, the galvanometer-driven x-y scanning mirrors will scan the beam across the sample, allowing for excitation of discrete areas (which will later be the basis for a pixel in the image) within the plane. Once an area is excited, the resulting fluorescent light travels back up through the objective lens and through an array of dichroic mirrors within the microscope. These dichroic mirrors, which serve as filters, enable us to fine-tune the system to choose the different signals we are interested in. For data collection with zebrafish, we generally use a 490 nm long-pass dichroic mirror for the first round of collection, which will reflect the autofluorescence signal

and allow the GFP signal to pass, and a 530 nm long-pass dichroic mirror for the second round, as illustrated in Fig. 7.

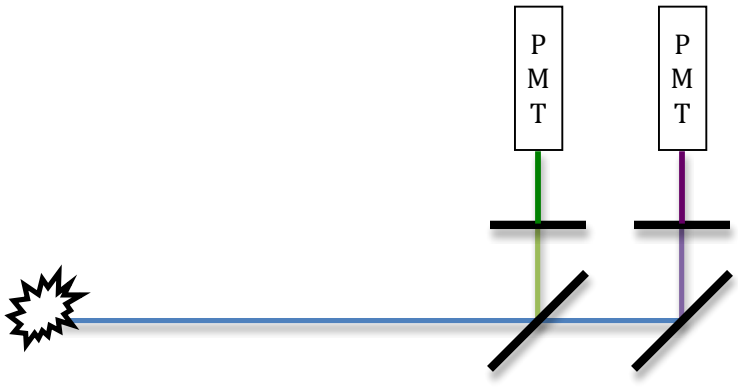

Figure 7. The fluorescence signal is collected and filtered by the dichroic mirrors. The first reflects the autofluorescence signal but allows the GFP signal to pass. The second reflects the GFP signal and lets anything else lower through. Each reflected signal is then filtered further by band-pass mirrors to a 25nm range of wavelengths for precise detection.

Once the light is reflected into the appropriate channel by the dichroic mirror, it passes through a band-pass filter, which serves to filter the light further into a particular range. The final, filtered signal is then coupled into a photomultiplier tube (PMT).

Data collection

In the PMT, the photons of light hit a semiconducting photocathode and in turn the photocathode emits electrons as a result of the photoelectric effect. These electrons then accelerate through a high potential, hitting a multitude of semiconducting dynodes along the way and causing these dynodes to emit other electrons via secondary emission. This process thus causes electron amplification with a gain often on the order of 10^6 to 10^9 electrons. At the end of the PMT, all of the electrons will hit an anode, causing a sharp current pulse with only a small delay (often on the order of a few nanoseconds). This current pulse will pass to a discriminator. The

discriminator works to filter pulses based on their amplitude, allowing only those above a certain threshold to pass. This process essentially works to filter out current pulses that are caused by background noise or other forms of insignificant signals. If the current pulse is determined to be useful by the discriminator, it is transformed into a TTL voltage pulse. This process (from the PMT to the discriminator) is followed for each pixel scanned. Since each pixel will release a certain amount of photons relating to the intensity (more photons make a higher intensity), then the discriminator can turn each current pulse generated by a photon into a voltage pulse, and all of these pulses can be collected for a certain pixel, allowing the acquisition of intensity values pixel-by-pixel. These voltage values can then be collected as a 256x256 matrix by a custom Labview program and displayed on the computer as a false-color rendering based upon the intensity of the image, as illustrated below. Essentially, the lowest voltage will be assigned a certain color and the highest assigned another, with the intermediate values being on a gradient between the two. Most of the time when we view the images, it is on a gray scale – white being the highest intensity and black being the lowest. Since this whole process is followed only for a single focal plane, we must repeat over a multitude of focal planes to get a 3-dimensional image. To do this, a computer-controlled z-scanner is used to scan down by a predetermined step-size (usually about 3 micrometers) after a plane is imaged, allowing the acquisition of a stack of images, each being a set distance apart. The end product of all this, then, is a set of .dat "images" that are ready to be viewed and processed using different types of software.

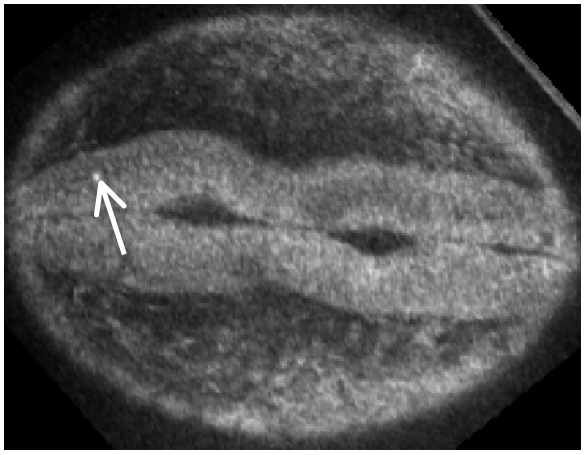

Figure 8. A typical image of the MHB. The image is formed by comparing relative intensities of the different pixels and assigning white to the pixel with the highest intensity and black to the pixel with the lowest. The rest are then scaled accordingly. The white arrow points to a white pixel, the highest intensity.

Image processing and data analysis

Once the image is collected on the computer, we must process and analyze it. This can be generally described in two steps – image conversion/processing and image analysis.

Image conversion and processing

The customized Labview program allows us to collect the image as a .dat file consisting of the intensities of each pixel. Using matlab, we can display the .dat file as a false-color gray-scale image based on relative intensities, as displayed above in Fig. 10. Since biological samples are non-uniform, some pixels will naturally have a much higher intensity than others. Since the false-color images are based upon the relative intensities, if there are large differences between two pixels, it may cause one to appear extremely bright and one to not really be visible at all. This can be quantitatively viewed by looking at a plot of intensities for each pixel, as shown in Fig. 9, given in photon counts.

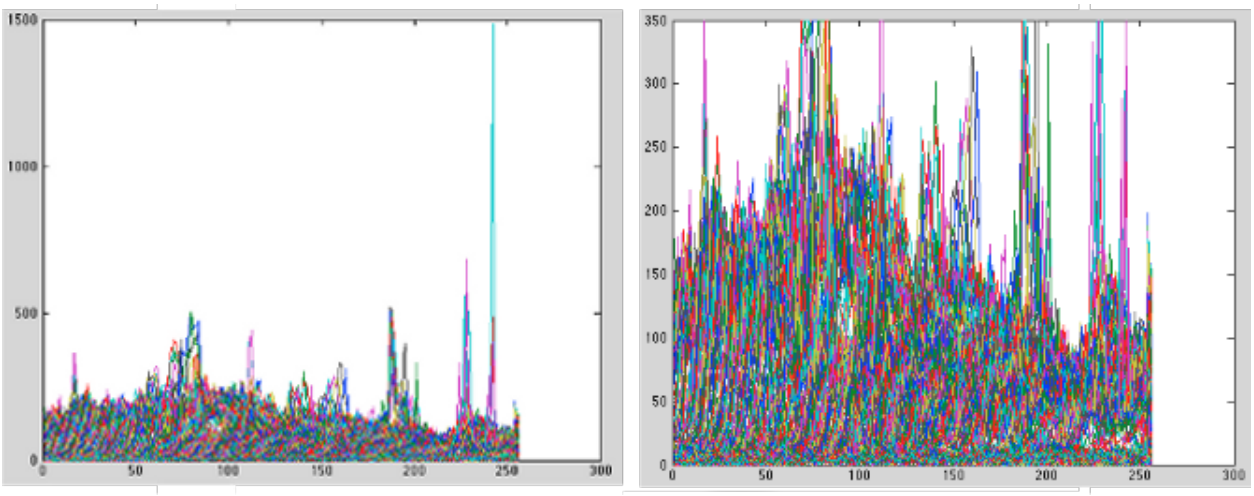

Figure 9. Plots showing the photon counts per pixel. Left: A non-adjusted intensity plot. The signal from a group of pixels toward the right is much larger than the signal from the others, causing the other signals to appear very weak. Right: A plot adjusted using "haircut". Now, all of the intensities are in a relatively close range, allowing for all pixels to be better visualized.

To fix this large variance in intensity, we can use a code in Matlab called "haircut". Essentially, haircut assigns a maximum intensity that each pixel is not allowed to exceed. The pixels below this maximum intensity will not be affected, but the ones above it will become saturated and forced down to the determined maximum intensity, now being displayed as white on the gray-scale image. An example of this is illustrated in Fig. 10 below.

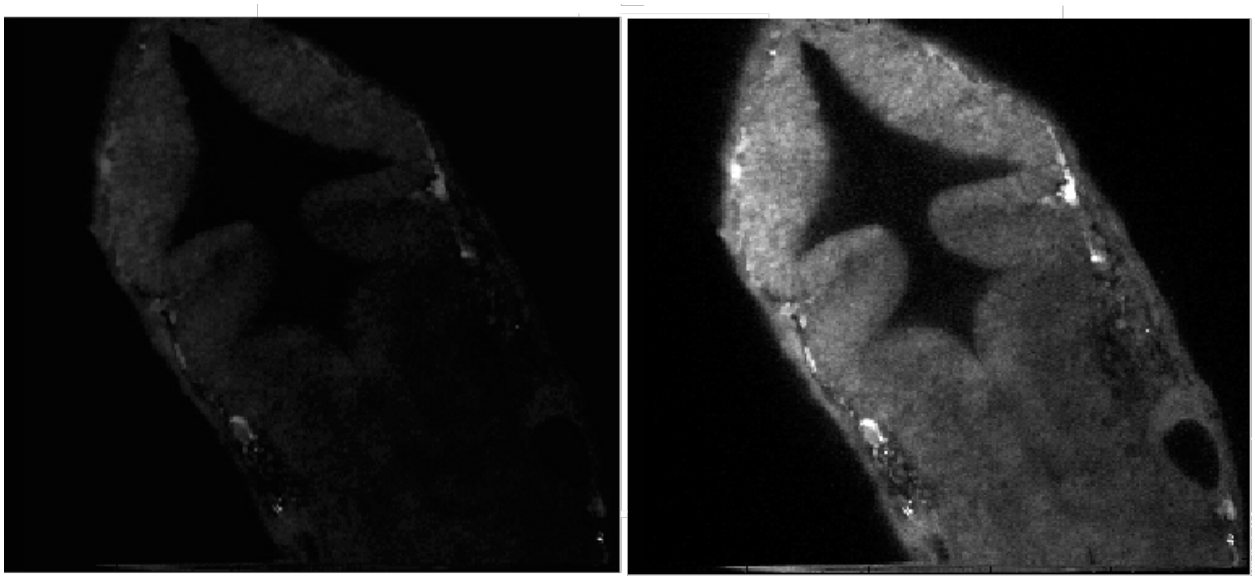

Figure 10. Left: An image before adjustment with "haircut". Right: The same image, now adjusted. These two images correspond to the plots shown in Figure 11.

Once it has been determined that the maximum intensity assigned is a good fit for our data, we can apply this rule to the whole stack of images. To do this, we use a custom code called "cut_n_stack" in Matlab, which takes the stack of .dat files that we have and applies the maximum intensity rule to each. It then saves these files in a ".tiff" format in a pre-determined folder. The final product, then, is a set of images that are properly processed and now ready to be turned into a full, 3-dimensional image stack.

To transform the set of images into a final stack, we use an open source program called V3D. Within V3D, we import the set of .tiff files we initially had and save them together as a stack, now allowing for 3-dimensional views, as shown in Fig. 11.

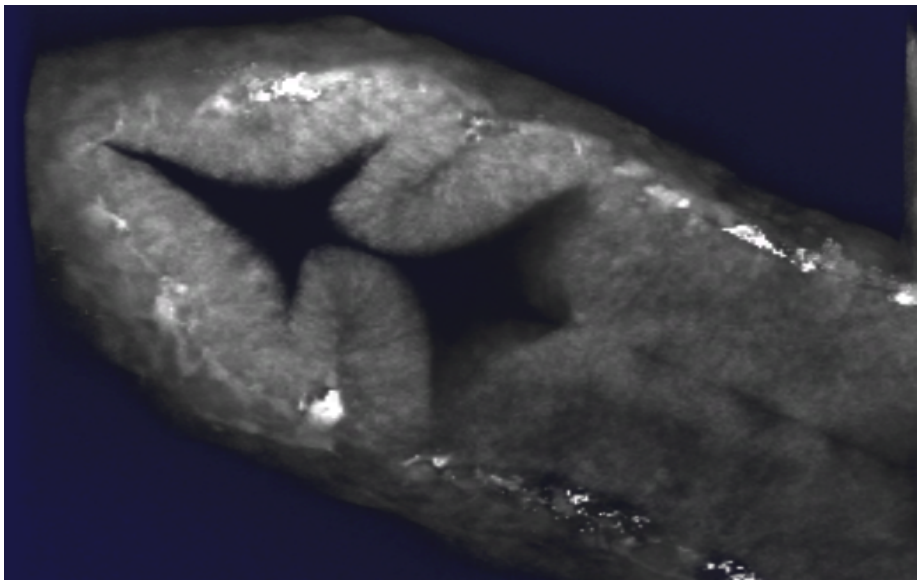

Figure 11. A 3-dimensional view of the MHD, depicted as if looking down from above.

We can then move to the final program used for image processing, called Fiji. Fiji allows us to view the image stack from the three orthogonal Cartesian views – x,y and z. When measuring the embryo, however, it is necessary to properly align the different areas of the embryo so that they

are lined up as if looking dorsally at the MHB. For instance, if one were looking straight down at an embryo from above, they would see the top of the head and the MHB – we align Fiji to make this view the x-y plane. If looking from a side (x-z plane), one would see the side view of the head; from the front (y-z plane) one would see the eyes and a cross sectional area of the MHB. We need to make sure the images in Fiji line up just like that – this is important both in visualizing the embryo correctly and when accurately taking measurements. Fiji has a built-in rotation tool, allowing us to rotate the embryo about the x,y and z axes, achieving the desired views. An example of a raw image stack vs. a rotated image stack is illustrated in Fig. 12.

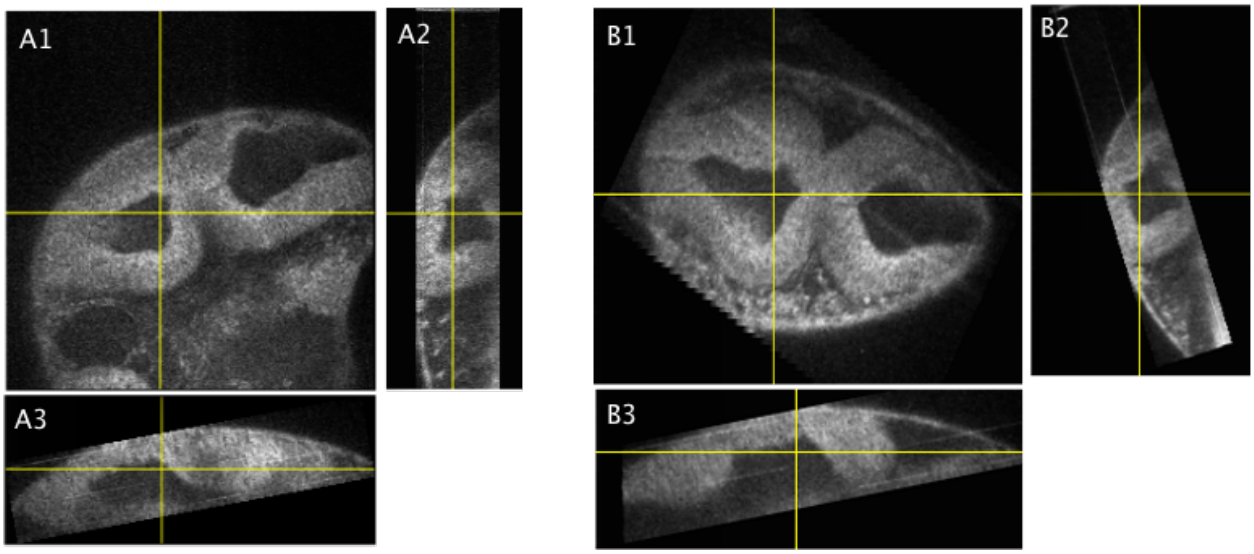

Figure 12. Left: Orthogonal views of an image stack before alignment. Right: The same image stack now properly aligned. A1 and B1 are in the x-y plane, A2 and B2 in the x-z plane, A3 and B3 in the y-z plane. Proper alignment is important in order to make sure that our measurements are consistent.

Data analysis

Now that the images are converted and transformed into a properly aligned stack, we can analyze the data that we have. Since each of the projects have different goals, each must be approached differently in terms of analysis. For the lineage restriction problems, we are simply interested in viewing whether or not the cells expressing GFP have crossed at the boundary. To

see this, we look at the image stack and observe the GFP-marked cells; no further data analysis is required. However, for the staging project, we needed accurate quantitative measurements of different parameters within the MHB. To make these measurements, we used the measuring tools within Fiji. These tools allow us to do various things such as measure an angle, measure a length or even measure an area of a selected space; all of length and area measurements are given in terms of pixels, and the angle measurement is in terms of degrees.

To keep consistency when collecting data, it is important to make sure that the same area is measured every time for a set of measurements. It is easy to see this in the x-y view, as many morphological markers, such as the constriction angle, are present. However, it is a little more complicated to find something reliable in terms of depth (on the z-axis). To fix this, I came up with the R-value. The R-value is the ratio of the depth into the zebrafish to the total depth of the zebrafish (down to the yolk), measured straight down from the MHBC. What the R-value does, then, is keep the same relative depth within the zebrafish embryo, even as it is developing. An example of the R-value is illustrated in Fig. 13. By using this parameter, I can make measurements at varying depths within the MHB over time, allowing me to accurately model how this area develops both spatially and temporally.

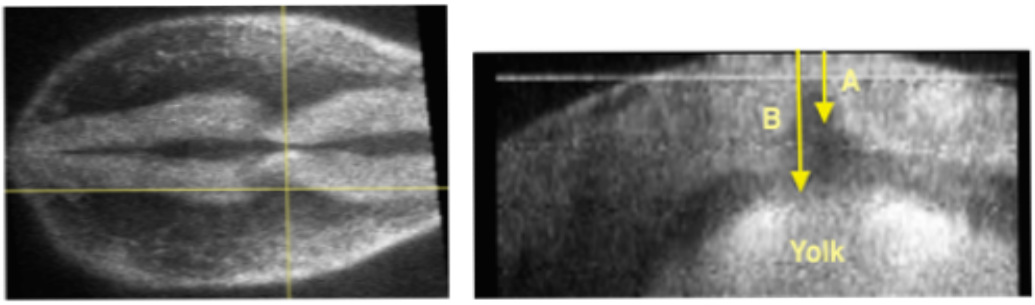

Figure 13. Images detailing the R-value. Left: To be consistent, I always move the crosshairs to the left side of the MHB and measure down from there. Right: The width ratio is A/B – the ratio of the depth within the embryo to the total depth down to the yolk.

As discussed previously, for the staging project I collected images of five different stages within the segmentation period – the 10,15,17,21 and 24 somite stages. For each stage, I collected at least three image stacks (each from a different embryo) and analyzed them. As well, to reduce statistical errors when taking measurements over an embryo, I took each measurement three times and took the average of these measurements. By analyzing the different parameters within these stages at the appropriate R-value, I was able to find a few parameters that are consistent throughout development of the MHB, allowing me to accurately describe and stage how this area develops, to be discussed in the results section.

CHAPTER III

RESULTS

Staging and modeling MHD development

To make a reliable biological model and staging system, it is important to be able to accurately describe a given stage of development with biologically relevant parameters. Such parameters may include anything that can be viewed across a variety of stages and samples and also develop at similar rates among different organisms within a species. For this project, I measured a variety of parameters within the MHB of the zebrafish, hoping to find something consistent and quantifiable throughout a range of embryos. I identified two parameters to measure: the constriction angle at the MHB and the ratio of the width at the widest part of the midbrain to the width at the actual constriction, as illustrated in Fig. 14.

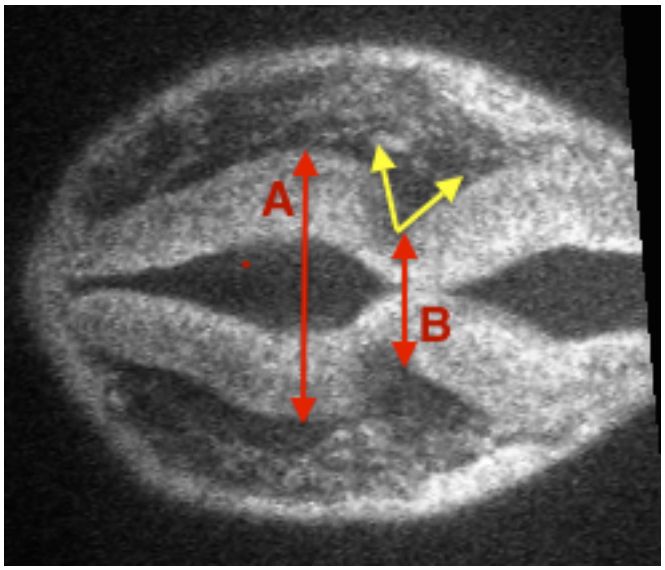

Figure 14. Yellow arrows: a measurement of the constriction angle at the MHB. Red arrows: the width ratio is B/A, the ratio of the width of the MHD at the constriction to the width of the widest part of the midbrain.

These parameters not only allow a quantifiable staging system, but they are also morphologically relevant, giving insight into how the tissue in this area folds and grows, both spatially and over time.

The Constriction Angle

The constriction angle at the MHB is important to study for several reasons. Since the boundary acts as a lineage restriction, studying the MHBC can lead to insights about how other lineage restrictions physically form. Also, understanding how the constriction forms over time can help to further understand the mechanical forces at play in the MHB.

My measurements revealed that the MHBC decreases steadily over time from about 180 degrees at 10 somites to 50-70 at 24 somites. To model the data, I used a linear least squares fit and found a relatively good fit, with a coefficient of determination above 0.8 for each depth. Raw data and charts are in Appendix A; illustrated below is a plot of the linear regression fits of the constriction angle development at the different depths.

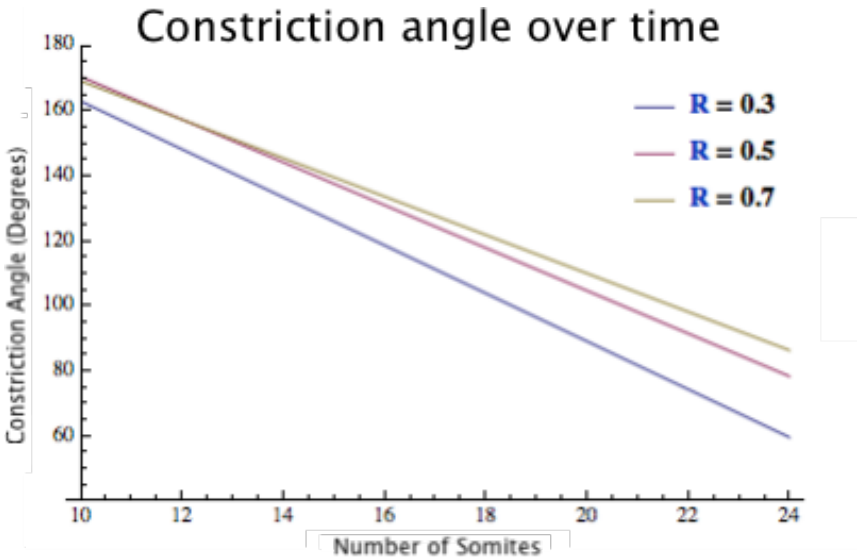

Figure 15. A plot of the constriction angle over time for different R-values. In general, the constriction angle decreases more slowly at larger depths. That is, it decreases quickest at R=0.3 and slowest at R=0.7.

As illustrated for the different R-values in the plot above, the rate of change of the constriction angle decreases as one goes deeper into the MHB. What this points to, then, is that it is important to study the constriction angle at all depths when studying the MHB since it is not the same throughout. As well, this indicates that conditions are not equal for every part of the MHB, indicating there may be different forces or mechanisms influencing different depths within it.

The Width Ratio

The width ratio, the ratio of the width at the MHB constriction to the width at the widest part of the midbrain, was found to be simpler to measure than the constriction angle. This is true because the images were more clearly resolved at the edges, leaving less room for subjective error. Since past studies have indicated that many of the cells actually shaping the constriction angle (predominantly by basal constriction) are present between the widest part of the midbrain and the MHB (Lowery 2008), understanding how they grow relative to each other can help to further understand the effect these cells have.

Similar to the constriction angle, I found that the width ratio decreases linearly over time. That is, the width of the MHB at the constriction gets smaller relative to the width at the largest part of the midbrain. However, unlike the constriction angle, I have found that the width ratio develops similarly at all of the different depths, changing by no more than 5% with depth, which can be explained by error within the least square fit.

The fact that the rate of change of the width ratio does not change much with depth indicates that similar mechanisms may be at play in shaping this at the different depths. As well, since this is

just a ratio and not definitive measurements, it is possible that the constriction width may be changing more while the midbrain width changes less, or vice versa.

The staging system

Since there is significant variability between different organisms even within a species (imagine humans at different heights) it is hard to make a staging system using only a single measurement. Thus, to make a more accurate system, I combined the measurements for the constriction angle and width ratio, leading to a relatively precise system that is able to accurately predict the age of the zebrafish to within plus or minus one somite, in contrast to the Kimmel staging system which is roughly one-somite intervals of staging. The most reliable data was generally at R=. 5, so this staging system is based on measurements at this depth.

To develop this system, I used some simple rules of probability. To start, I picked ranges for the different stages and measurements. For staging within plus or minus one somite, I broke the stages into 10-12, 13-15, 16-18, 19-21 and 22-24 somites. While also keeping relatively good accuracy (being accurate to within an hour of development) it also perfectly fit the spread of stages from which I originally took data, including one in each category. Next, I broke the measurements up into categories – for the constriction angle ranges of 25 degrees and for the width ratio ranges of 0.1. Once the data was broken into categories, I essentially made charts of when these different measurements overlap for different stages and found that they only overlap at very specific times. The resulting system is illustrated below. So far, it has passed validation tests using an unknown embryo as well as having someone else taking measurements to rule out subjective bias.

Width Ratio \ Constriction Angle	180-155	154-130	129-104	103-78	77-52
1.0-0.9	10-12	X	X	X	X
0.89-0.79	X	13-15	16-18	X	X
0.78-0.68	X	13-15	13-15/16-18*	19-21	X
0.67-0.57	X	X	19-21	19-21	X
0.56-0.46	X	X	X	22-24	22-24

Table 1. The staging chart. To find the range of stages the embryo is in, one simply needs to measure the constriction angle and width ratio at R=0.5. From there, he or she can look at this chart and be given the range of stages the embryo is in. In the starred box, there is a 50% probability that the embryo is in either of these stages. For all other boxes there is 100% probability.

Lineage restriction

The lineage restriction project has focused on determining whether actomyosin causes cells to be restricted or to cross at the lineage boundary in vertebrates. This project was relatively straightforward in testing our hypothesis. If we observed cells proliferating across the boundary when Blebbistatin was applied, it means that actomyosin cables played a role in subduing these movements. If nothing happened, then there are mostly likely other mechanisms reinforcing this. So far, our preliminary results indicate that actomyosin cables do indeed play a role in the lineage restriction at the MHB; however, further studies will be needed to verify. As illustrated, we visualized the GFP-marked cells being restricted in a control embryo but proliferating across what was previously the lineage restriction in a treated embryo. s

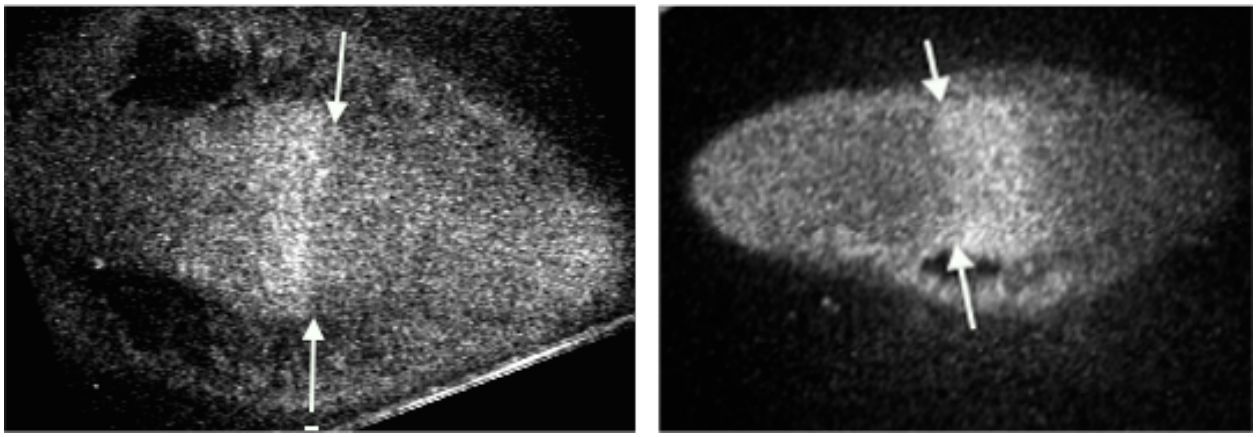

Figure 16. Images of the GFP-marked wnt-1 cells at the lineage restriction. Left: An embryo in the control group. Right: A Blebbistatin-treated embryo, this image shows the GFP-marked (brighter) cells proliferating across the boundary. White arrows mark the location of the boundary. Each embryo is at 15 somites and was fixed according to protocol explained earlier.

These images suggest that the Blebbistatin did have an effect in stopping the lineage restriction formation in this area. To be certain of what actually happens, however, further studies with better-quality images and time-lapse data are necessary.

CHAPTER IV

DISCUSSION

The capability of UPM to allow visualization of things not otherwise possible in biological specimens makes it a unique and very useful imaging system. While other biological methods, such as *in-situ* hybridization, may allow visualization of both genetic and structural components, they do so usually at the cost of the embryo's life. Since UPM allows *in-vivo*, multimodal imaging of an embryo, it can be invaluable for studies in which samples must be alive and in a natural environment.

UPM is important for studies of how the MHB forms because the MHB is naturally a 3-dimensional structure, changing in shape and size at different depths. While the UPM system is very good for taking high-quality images, there will always be some experimental error involved, often leading to imperfect images. For instance, improper pulse shape or not being at the ideal output power could affect the extent to which we excite the sample. Improper calibration of the dispersion-compensating mirrors could lead to the pulse experiencing more residual dispersion than expected, again leading to non-ideal excitation of the sample. Additionally, the photomultiplier tubes are consequentially very sensitive to ambient background light since they must be so sensitive to gather the fluorescence signal from the embryos. Thus, signals often have noise associated with them, coming from things such as the laser speckle reflection off of the wall or components, or light shining into the dark room from the crack under the door. Also, there may be some error associated with things other than the actual system. For instance, many of the times I took images, the embryos ended up being damaged not by the system itself but by the process of mounting it in the agarose gel. The agarose gel, as well, will cause a large amount

of scattering if too much is placed on top of the embryo, leading to a weaker signal and thus a lower signal-to-noise ratio. Due to errors such as these, many of the images I collected were imperfect. These imperfections led to error in the measurements and the necessity to specify a range of error in the measurements, highlighted in Appendix A. However, despite the error present, UPM still allowed for high-resolution images of the MHB and for the 3-dimensional visualization that would not be possible with other systems.

Due to the error-limited measurements and also the variability among the different embryos at the same stage, I was only able to break the staging system into groups of three somites, allowing for one-hour time resolution. I was able to do this with three embryos per stage, so my next goal is to get images of ten embryos per stage, hopefully leading me to be able to resolve single-somite stages within the development using the MHB, allowing me to match the time periods resolved in Kimmel's staging system. For this project, my biggest challenge was in actually mounting the embryos to image them. Each embryo only takes roughly twenty minutes to image, and I usually image in three hour sessions with the goal of getting an embryo imaged every twenty minutes, meaning nine embryos per imaging session, ideally. However, due to complications in mounting the embryo inside of the well, I am usually only able to get three embryos at max over a three-hour time span, leading to a vast reduction in the amount of data I would have in an ideal situation.

For the lineage restriction project, UPM allowed me to properly visualize previously restricted cells proliferating across the MHB lineage restriction in a treated embryo. While this is great to see, there is still much data to be taken. Unfortunately, for this study, the biggest limitation was

the actual production of embryos. I generally set up the transgenic (GFP-marked) zebrafish to mate and produce embryos two to three times per week over an eight week span, but only got four rounds of embryos with which to experiment. As well, the number of embryos produced by the transgenic zebrafish when they did mate was significantly less than the amount produced by wild-type zebrafish. Also, much of the time spent during my time working with this project was in titrating to find the right amount of Blebbistatin needed for an embryo to be affected without being harmed by the DMSO that the Blebbistatin was dissolved in. Despite these limitations, my next goal is to take more images of cells proliferating across the lineage restriction (and also images of the control group) and to find when exactly the mechanisms leading to this lineage restriction begin to act.

The entire goal of these projects is to be able to describe (mathematically and biologically) how the lineage restriction at the MHB forms, and how the MHB itself forms. Understanding this process in depth is important because both lineage restriction formation and MHB morphogenesis give rise to many important and fundamental biological structures. By increasing the precision and temporal resolution of the staging and modeling project and by further understanding what leads to the lineage restriction formation and when these processes start, I can go further toward this goal. However, other studies will probably be needed as well.
If time permits in my undergraduate career, I plan to use UPM to further the understanding of other physical mechanisms that give rise to the MHB. For instance, understanding how cellular structure influences this formation and what exactly it does can further this model. This can be visualized with membrane-bound GFP or simple membrane dyes. As well, I can stain the

extracellular matrix of these cells and look at the structure to see if it may play any role in establishing the lineage restriction or overall morphology of the MHB.

While biological systems such as the MHB are inherently complex, a reductionist approach can lead to significant insights and understanding. UPM allows us to do this – it allows visualization of the individual components – cells and their structures – alongside what causes them to work. Thus, UPM can help guide researchers in understanding biological phenomena such as this formation and hopefully to a fuller understanding of how this can be used to benefit human health as well.

REFERENCES

Barkovich, A. J., et al. (2009). "A developmental and genetic classification for midbrain-hindbrain malformations." Brain **132**: 3199-3230.

Gibbs, H. C., et al. (2013). "Imaging embryonic development with ultrashort pulse microscopy." Optical Engineering **53**(5): 051506-051506.

Kimmel, C. B., et al. (1995). "Stages of embryonic development of the zebrafish." Dev Dyn **203**(3): 253-310.

Landsberg, K. P., et al. (2009). "Increased cell bond tension governs cell sorting at the Drosophila anteroposterior compartment boundary." Curr Biol **19**(22): 1950-1955.

Monier, B., et al. (2010). "An actomyosin-based barrier inhibits cell mixing at compartmental boundaries in Drosophila embryos." Nature Cell Biology **12**(1): 60-U147.

Peter T.C. So, B. R. M. (2009). Handbook of Biomedical Nonlinear Optical Microscopy. USA, Oxford University Press.

APPENDIX A

CHARTS AND GRAPHS

R=0.3

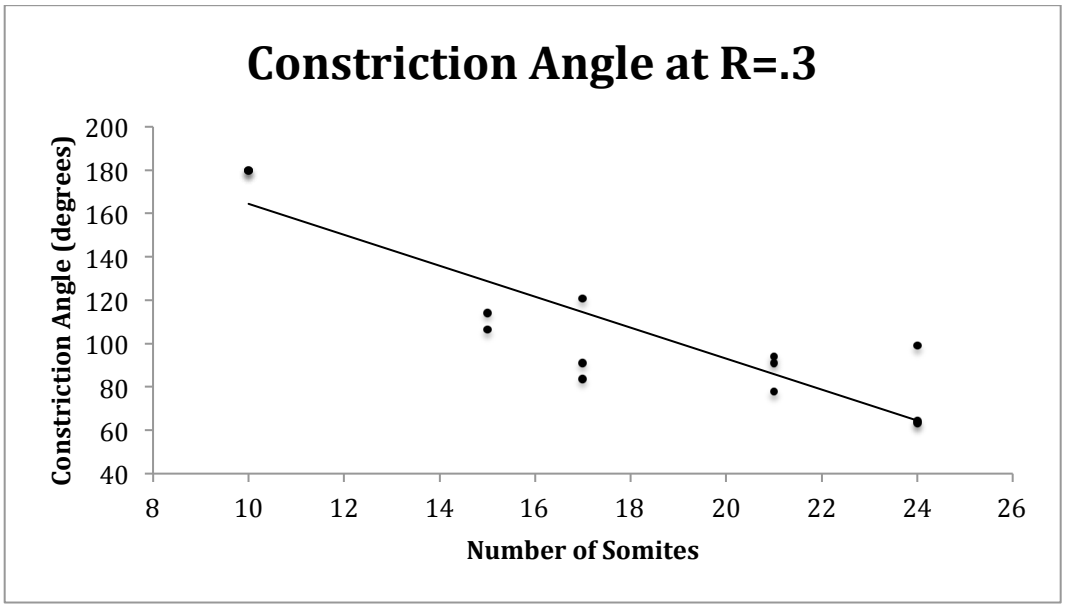

Linear Least Squares Fit: y= -7.38x + 236.8 | R^2 = 0.90 | Slope Uncertainty =0.90

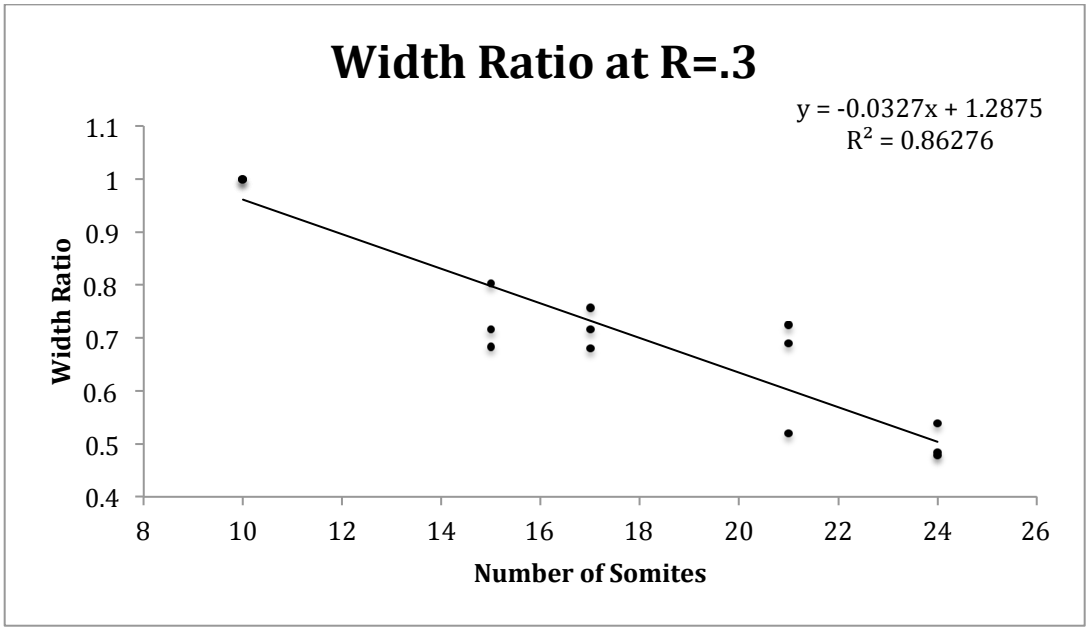

Linear Least Square Fit: y=-0.033x + 1.29 | R^2 = 0.86 | Slope Uncertainty = 0.004

R=0.5

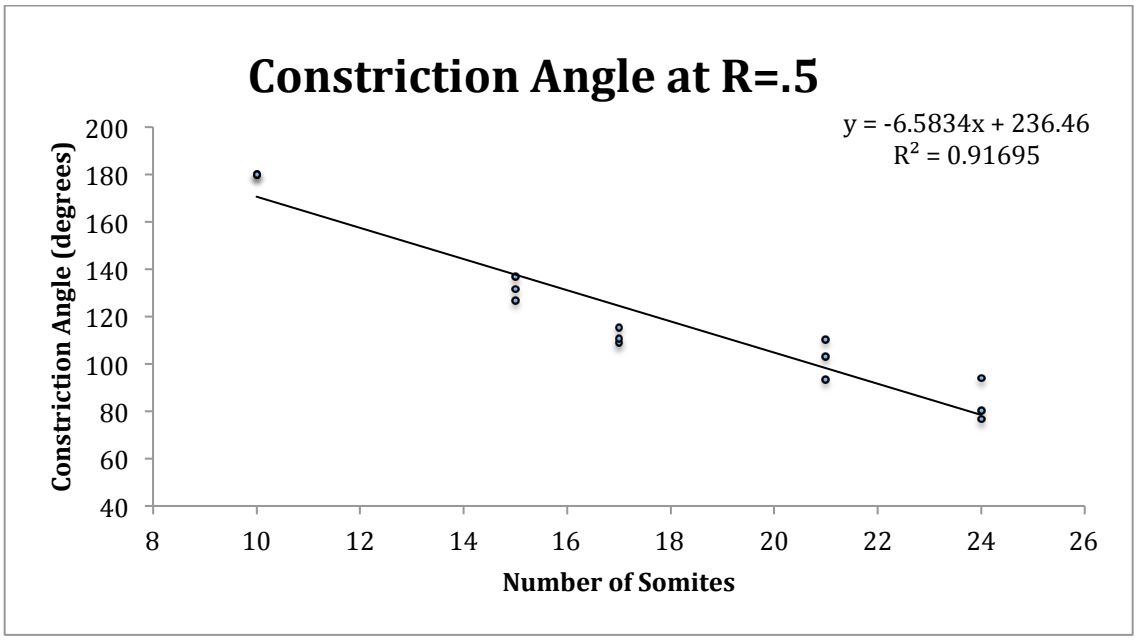

Linear Least Squares Fit: y=-6.58x + 236.4 | R^2 = 0.92 | Slope Uncertainty = 0.55

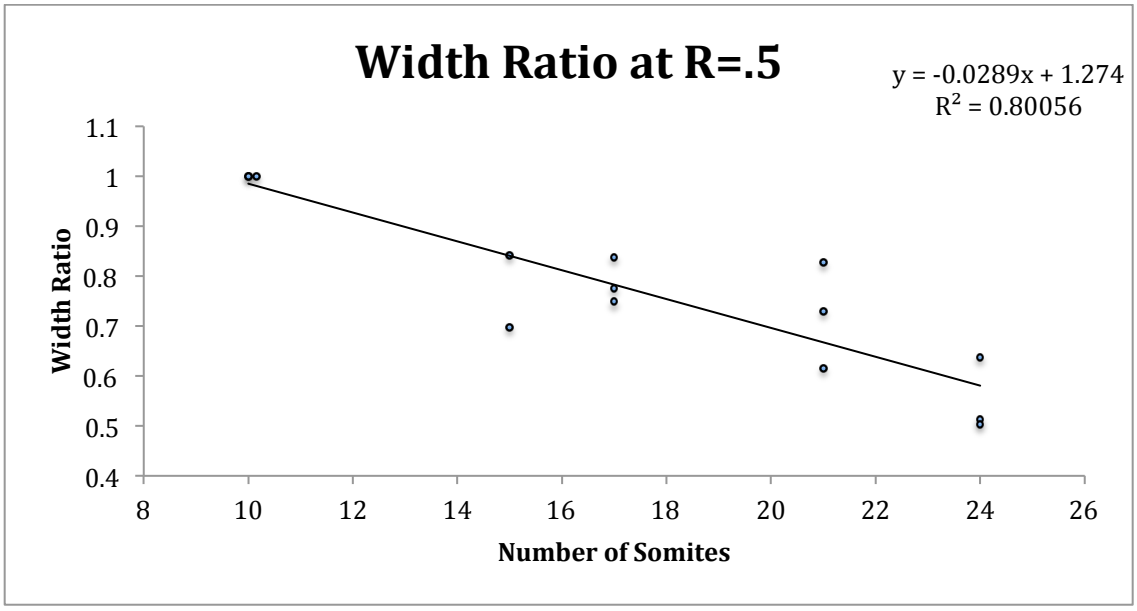

Linear Least Squares Fit: y= -0.032x + 1.303 | R^2 = 0.89 | Slope Uncertainty = 0.003

R=0.7

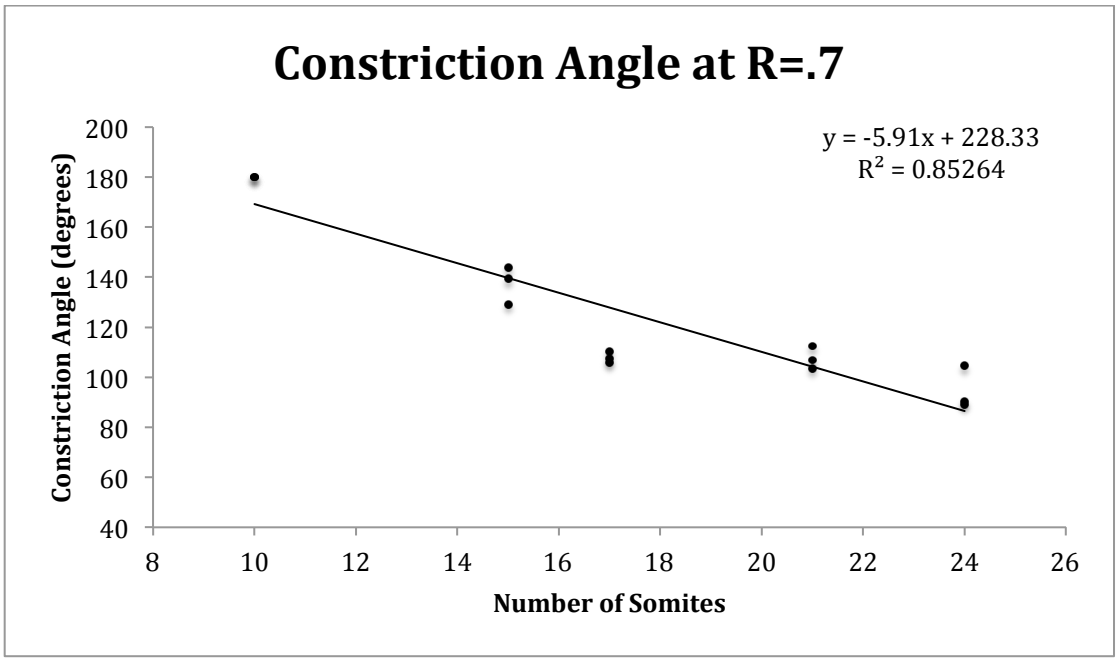

Linear Least Square Fit: y = -5.91x + 228.3 | R^2 = 0.85 | Slope Uncertainty = 0.68

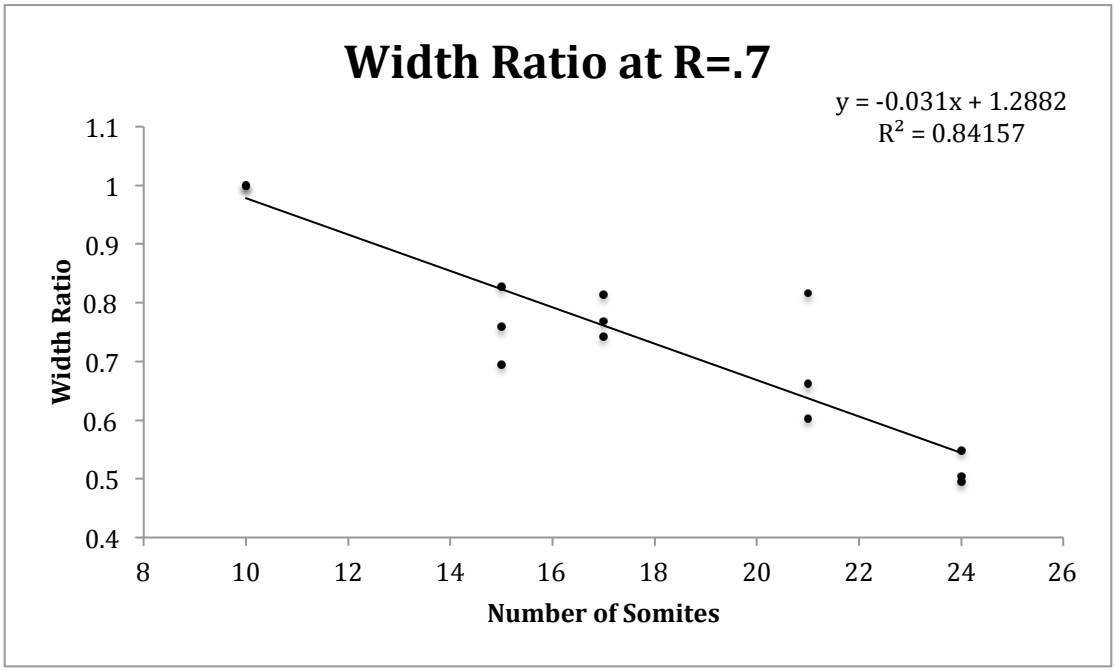

Linear Least Squares Fit: y = -0.032x + 1.306 | R^2 = 0.845 | Slope Uncertainty = 0.004